

GNSS Expected Performances in Earth - Moon Trajectories

Giovanni B. Palmerini, *DIAA - Università di Roma La Sapienza*
Marco Sabatini, *DIAA - Università di Roma La Sapienza*
Giorgio Perrotta, *Istituto Italiano di Navigazione*

BIOGRAPHY

Dr. Giovanni Palmerini is professor of Aerospace Guidance and Navigation Systems at Sapienza Università di Roma, and teaches Aircraft Navigation at the Università di Bologna.

Marco Sabatini is research assistant at Sapienza – Università di Roma. He got his PhD in Aerospace Engineering (2008) with a thesis on Formation Flying Dynamics and Control.

Giorgio Perrotta, vice president of I.I.N., has a long experience in Selenia and Alenia. He is currently the owner and manager of SpaceSys, a small-medium enterprise active in applied research and design in the aerospace field.

INTRODUCTION

Interest for lunar exploration spread off recently, with and a sounding perspective of an increasing number of spacecraft en route to the Moon in upcoming years. There is actually a strong difference between this return to the Moon and the pioneering exploration of the '70s, as the current initiative poses a special emphasis on several, cost-efficient missions exploited by means of small platforms. In such a perspective, a remarkable difference is in the guidance, navigation and control function. In fact, it is unlikely that these small mission can benefit from a continuous, expensive control by a network of ground based stations. Instead, a large level of autonomy, allowed for by recent technology developments, should be targeted. Of course, any guidance and control should start from a correct knowledge of the kinematic state of the spacecraft. A chance to increase the autonomy with respect to these knowledge should be given by leveraging to lunar transfer the technique which is becoming a standard one in Low Earth Orbit spacecraft, i.e. the use of satellite-based navigation systems (GNSS). Beginning with code, and

extending to phase observable, a number of applications ([1],[2]) validated this approach, leading to a not negligible market for space-qualified receivers. There is even a growing trend in considering GNSS even for attitude evaluation. Other attempts investigated and actually tested the possible application to orbits higher than MEO, where the transmitting GNSS spacecraft are located ([3], [4], [5], [6]). The strong asset for all these cases is represented by the limited impact (mass, volume, and, for positioning, also power) the receiver presents with respect to on-board hardware, with the location of antennas as the only serious issue to be negotiated depending on the specific spacecraft foreseen attitude evolution.

Within such a perspective, it is obvious the interest to deeply analyze the possible application of the same technique to lunar transfer. As in the case of HEO and GEO orbits, receiving antennas will be basically working in a look-down configuration, as no sources are presently located above a MEO altitude of about 20000 km. The signal is represented by the spill-over all around the Earth figure of the main lobe (beamwidth amplitude for GPS is about 28°) irradiated by satellites servicing the opposite hemisphere of the Earth. Additional signal is provided by secondary lobes of the GNSS satellites servicing the same Earth hemisphere the spacecraft is flying over. Low signal level due to the dependency on the square of the distance of this available signal, if any, makes the acquisition quite difficult and spaced out by frequent outage periods. Even if the acquisition is successful, the quite poor geometric dilution of precision factor leads to a coarse solution in terms of accuracy.

This scenario was investigated in [6] with reference to ESMO (European Student Moon Orbiter), a mission concept initially developed by SSETI and ESA. The analysed long duration transfer (see also

the next paragraph) allowed to evaluate the magnitude of outages' effect, considering both the GPS and the GPS plus Galileo as GNSS sources. In a following development [7] the advantage of relaxing the constraint on the continuous availability of a fix was stressed. In fact, an estimator, built thanks to the good knowledge of the dynamic environment, can easily fill the intervals where no signal is available, confidently propagating the state. Results in [8] were referred to a direct, short duration transfer, with GPS as the only source. Main task of this analysis was to assess the performance level of the GNSS navigation technique, intended as the error of the estimate in position and velocity, especially at the critical time of the injection in the sphere of influence of the Moon and at the time of possible manoeuvres to attain a lunar orbit of interest.

With respect to previous papers by the same authors ([7], [8]), the present work extends the simulation inside the lunar sphere of influence up to the possible recircularization orbit. Moreover, full extent of the advantages of software receivers is included, by referring to a recent publication by Ziedan [9] where extremely low threshold values achievable with digital signal processing have been reported. The meaning of the simulations has been increased by improving the dynamical model considered, where third body perturbation has been explicitly included. In order to manage the dilution of precision, a first look has been given to the possible improvement in performance granted by a pseudosatellite located on the Moon, a concept which is gaining its way in the frame of the lunar exploration initiative. The final section with the remarks on the simulation results points out the current status of the investigation and indicates selected additional steps in such a line of research.

MISSION SCENARIO

Following the issues reported in the introduction, the case study which is deemed of interest for the present work is represented by a limited budget small platform, with reduced onboard availability of volume and power resources. With respect to navigation function, it does translate in a limited number of un-steerable GNSS receiving antennas, a constrained computing capability, and the lack of RF and optical sensors to offer a redundancy and back-up during the foreseen GNSS outages. A sketch of the platform (from [7]) has been reported in Figure 1 to show the antennas' configuration considered in the present work. The antennas are located on four sides of the spacecraft out of six, with the two panels along the nominal velocity

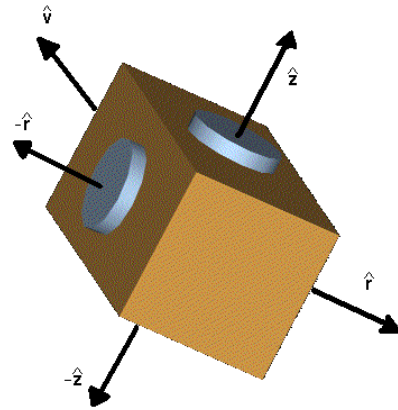


Figure 1 – Location of the four GNSS receiving antennas on the spacecraft.

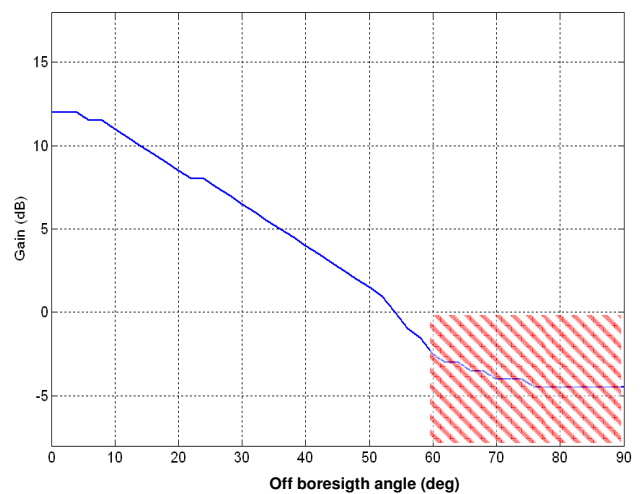


Figure 2 – The irradiation pattern considered for each of the 4 antennas on the spacecraft.

direction which are left completely empty for thrusters' nozzles. The radiation pattern admitted for each of the antenna has been defined on the basis of typical GNSS antenna performances [5], and is represented on Figure 2. A threshold for signals impinging at angles higher than 60° has been added to conservatively taking into account disturbing effect from satellite structure and payload optical/radiating heads. Of course, such a location and radiation pattern cause a dependency of the signal receiving capability and therefore on the proposed results on the attitude assumed by the spacecraft. In the following the spacecraft maintains a body axis constantly directed along the tangent to the trajectory, i.e. along the velocity direction. One of the other axes (the "r" in figure) will belong to the orbital plane, and the third one will therefore results parallel to the normal to the plane. The sources are represented by the GPS constellation alone, with 30 PRNs active and the relevant

ephemerides assumed according to week 388 almanac. The structure of the irradiated beam is the one of the Block IIR spacecraft, and only the main two lobes will be considered (see also [7] for detailed data).

With respect to the trajectory, different possibilities for lunar transfer do exist. Beginning with a classical LEO parking orbit to perform spacecraft commissioning, the simplest option is represented (Figure 3) by the injection on a transfer elliptic orbit, with an apogee which has the order of magnitude of the lunar orbit radius. Close to the apogee, there will be the insertion in the lunar sphere of influence (with the triangle of velocities represented in Figure 4), and then the descent towards the Moon and the acquisition of the targeted lunar orbit. The drawback of this strategy, which is labelled as *direct transfer* is represented by the high thrust phase at the insertion in the ellipse, while the advantage is given by a comparatively short travel time, which will be shorter as higher the impulse at the perigee. A variation of this approach provides the *free return* trajectories, largely investigated in relation to early '70s manned missions, as they will provide the chance to stay on track and achieve a re-entry option to the Earth if lunar descent phase should not be accomplished for technical reasons.

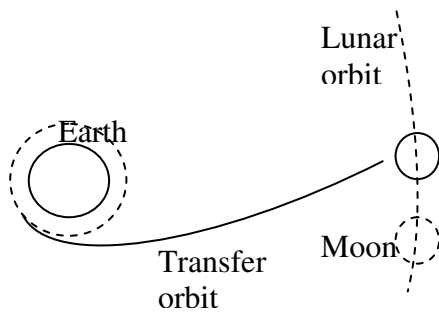


Figure 3 – A sketch of a direct transfer trajectory, from the parking orbit to the insertion in the lunar sphere of influence.

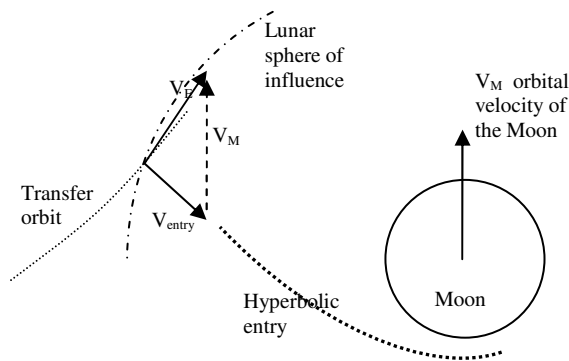


Figure 4 – Velocity triangle at the lunar insertion and lunar entry (hyperbolic) orbit.

A totally different possibility is represented by a low thrust spiralling in the Earth sphere of influence, moving away from the Earth, up to the insertion in lunar phase. Such a very long time transfer gained interest in recent years due to its compliance with the characteristics of electric propulsion, and has been used, as an example, for ESA's SMART-1 mission. Figure 5 reports a sketch of a lunar low thrust transfer initially considered for ESMO.

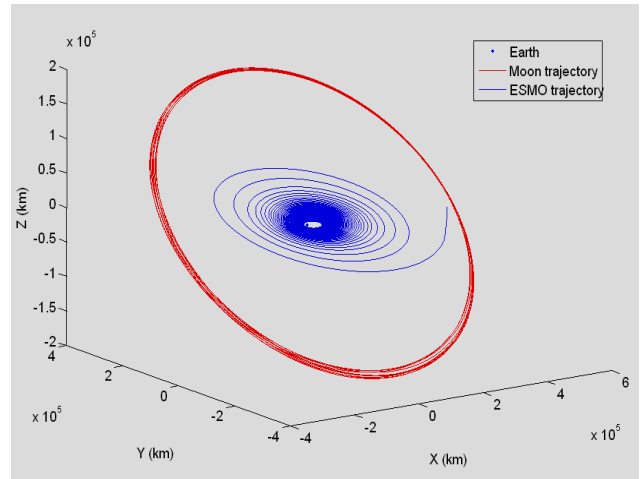


Figure 5 – A sketch of a spiralling, low-thrust, long duration transfer to the Moon (from [7]).

Finally, weak stability boundary transfer make a deep use of the non keplerian dynamics which actually better depicts the Earth-Moon system and the remarkable presence of an additional gravitational attraction from the Sun. The spacecraft points at first about 1 million km far away from the Earth body, at the boundary of the sphere of influence of the Earth-Moon system. Then, by making a savvy use of the gravitational pull of the Sun, with a really limited Δv it plunges into the lunar sphere of influence. Figure 6, from an ESA report for the ESMO mission [10], offers a sketch of an example of WSB transfer where the spacecraft is sent out up to the L1 Lagrangian point of the Sun-Earth system before coming back to the Moon. The main appeal of such a strategy is the limited thrust needed, while duration and operational issues are significant disadvantages.

Above all, these strategies are completely different from the point of view of navigation. In fact the extreme distance from the Earth attained during the WSB transfer clearly make impossible the GNSS-based technique in that case. Instead, both the direct and the low thrust transfers seem suitable for GNSS application, even if the limited number of manoeuvres required in direct transfer should greatly help in the preliminary assessment of the

visibility of the transmitting satellites at crucial times along the trajectory.

In order to point out significant result, the easier-to-compute direct transfer trajectory will be used in the following. Moreover, a simplifying hypothesis of the patched conics method will be used to design the tour. Therefore, the spacecraft will be considered as subjected to the keplerian attraction of one single body at the time: namely the spacecraft, following the insertion in the transfer orbit from the parking one, will stay on an ellipse until the boundary between the spheres of influence will be reached. The radius of the lunar sphere of influence is given by the relation (Lagrange)

$$R_{Msat} = D_{Earth-Moon} \left(\frac{m_{Moon}}{m_{Earth}} \right)^{2/5}$$

where D indicates the distance and m the masses.

Then, the only attraction will be the lunar one, and the spacecraft will be on a hyperbolic orbit until attaining the periselenium. The periselenium marks also the end of the transfer mission, due to the fact that it should be considered also the point to exploit a circularization manoeuvre to reach an observation orbit which is meaningful from the scientific point of view. The parameters for the selected trajectory will be as follows: parking orbit (and perigee) altitude is 318 km and eccentricity of the transfer orbit is 0.977. Insertion in the lunar sphere of influence arrives after 50.2 hours from perigee impulse, and the total time up to periselenium is slightly less than 65 hours. The trajectory is completely planar, with an inclination equal to the one assumed for the Moon, i.e. 23° from the Equator; the orbit of the Moon is considered as circular, with a radius of 384400 km.

SIGNAL AVAILABILITY

Actual availability of the signal in a really marginal condition as the one to be faced during the lunar transfer certainly depends on the capability to acquire an extremely weak signal due to the distance from the sources. The power received can be evaluated as

$$P_r = EIRP + G_t(\eta) + L_D + G_r(\delta)$$

where the terms represent the equivalent isotropic radiated power, the transmitting and receiving gains as function of the line-of-sight angles with respect to the transmitting and receiving antennas, and the free-space loss (see also [7] for details).

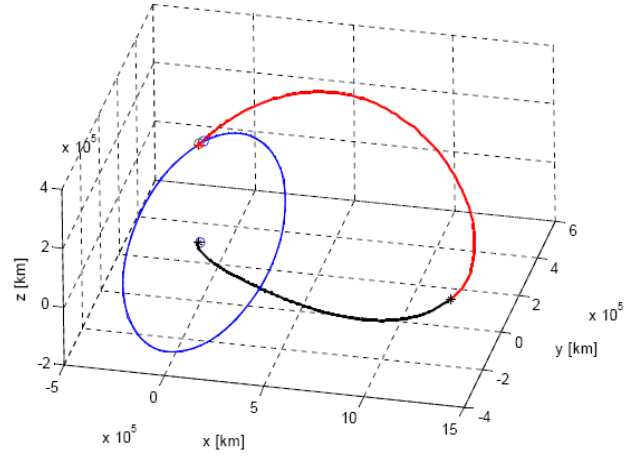


Figure 6 – Example of a Weak Stability Boundary (WSB) transfer trajectory from GTO to the Moon (from [11]). The black line depicts the trajectory from GTO to Sun-Earth L1, the red line the L1-Moon portion, while the blue line is the lunar orbit. Notice the scale with respect to previous cases.

The received power has to be compared with the noise level ($T_{sys}=190K$ is the noise temperature of the system, $L_{Nf}=-3dB$ is the noise figure of the receiver, $L_I=-1.5dB$ is the implementation loss – selected values are compliant with test experience reported in[6]),

$$SNR = P_r - 10 \log_{10} T_{sys} + 228.6 + L_{Nf} + L_I$$

to provide the final figure which should be compared with the signal acquisition threshold to validate the signal availability (see also next paragraph).

However, the capability to acquire the signal does not mean that the obtained solution will be accurate. In fact, the approximated relation

$$\sigma = GDOP \times \sigma_{URE}$$

underlines the relevance of the geometric dilution of precision (GDOP) factor as an amplification of the error in ranging measurements. GDOP becomes extremely high for an observer en route to the Moon, as its portion of the field of view including the sources shrinks. The value of the ratio between the diameter of GNSS orbits (about $5 \cdot 10^4$ km and the distance attained from the Earth (about $35 \cdot 10^4$ km) provides the required explanation. While acquisition threshold could be lowered by technical improvements, the geometry still represents a serious limit, and should not be completely solved even by including upcoming GNSS systems, which

will be still largely based on MEO. In order to manage such a constraint it has been proposed to locate a (network of) pseudosatellite on the lunar surface. The effects of such a choice will be preliminarily investigated in the following simulations, including for comparison a test with one lunar pseudosatellite.

SIGNAL ACQUISITION

The marginal level of the available signal calls for a solution which aims at minimum thresholds level for both the acquisition and tracking. The knowledge of the code used in the present and upcoming GNSS systems operating in a CDMA scheme (all of them with the exception of GLONASS to be probably corrected later) suggests to increase the correlation capability by processing longer – and variable - slices of the signal, a solution which can be provided in a easier way with a software processing. Furthermore, a software based receiver is especially suitable to change the acquisition and tracking process depending on the specific dynamics, and therefore to switch among different modes during the phases of the mission.

The software receiver allows for selecting a number of processing algorithms. In the present work, the threshold values used in simulation are 15 and 20 dB-Hz, remarkably better than a 30dB-Hz which should be considered a typical value for a classical hardware receiver. These figures for processing algorithms have been selected by check of results reported in reference [9].

Of course extensive correlation, either in time (as in the hardware case) or preferably in the frequency domain, requires a significant computation amount. It could be considered as a characteristic opposite to the preliminary requirement of very limited resources in board. However it has to be considered that the fix is not needed at the typical 1 Hz rate. Instead, the knowledge of the dynamic environment allows for carefully modelling and therefore leads to the adoption of estimators which are able to provide the spacecraft kinematic state (velocity and position) with high confidence even without measurements at the current time (see also the next paragraph).

A major drawback of the software tracking is represented by the fact that the signal is modulated also by the data message, with unforeseen bit values switches. Such a problem should be clearly taken into account and ends up in a constraint for the tracking algorithm. Help in solving such a bottleneck could be given by the presence of a pilot (i.e. data message – free) signal in the upcoming Galileo system [12].

KINEMATIC STATE ESTIMATION

The combination of poor signal level, changes in the sources geometry as the GNSS platforms move along their orbit, and variations in the attitude of the lunar-bound spacecraft leads to a number of intervals where less than four satellites are in view and the fix is therefore impossible. However the slow dynamics of a lunar transfer, together with the good knowledge of the dynamic model allow for a fruitful use of recursive estimators like the Kalman filter. Specifically, the Unscented Kalman filter (UKF, [13]) has been adopted for the present investigation, mainly on the basis of numerical considerations. In fact, the computation load (one of the drawbacks of this solution) is not a problem during simulation. Instead, computation of Jacobians (typical of the more popular Extended Kalman filter) is substituted by recursive evaluation of the dynamics, making by far easier any change in the model included in the filter. Details of the application to the present case are extensively reported in [8].

SIMULATION

Following figures reports the results of simulations carried out for different SNRs receiver threshold, and all of them are referred to the nominal direct transfer trajectory introduced in previous paragraphs. All runs, despite of the acquisition capabilities, led to remarkable GNSS outages, and the estimation between following available fixes has been carried out with the UKF. The relevant dynamics modelled into the filter includes the main attracting body (the Earth in the first part of the transfer, and the Moon in the second one) and the third body attraction, which is the leading perturbation. The Earth oblateness, the higher harmonics of the lunar potential, as well as other perturbations, like the solar radiation pressure, are not detailed at this stage, but taken into account in the filter as noise process. Due to the nature of these perturbations, the assumption of Gaussian nature can be accepted also with respect to the central limit theorem.

It has to be outlined that, due to the preliminary level of the present study, no effort has been devoted to optimize the filter by means of a careful tuning. Therefore, standard values currently used for GPS have been assumed for the standard deviation of the user equivalent ranging error. These values have been multiplied by a mid course GDOP to obtain the uncertainties of the sensor measurements (position and velocity given by GNSS). Initial guess

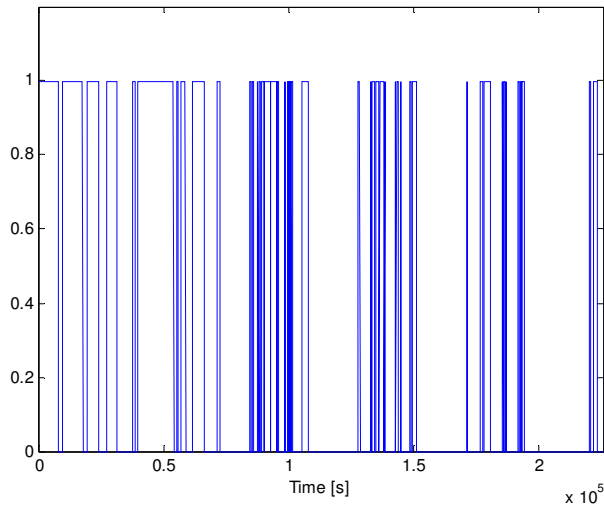


Figure 7 – Visibility flag (30dB-Hz threshold case)

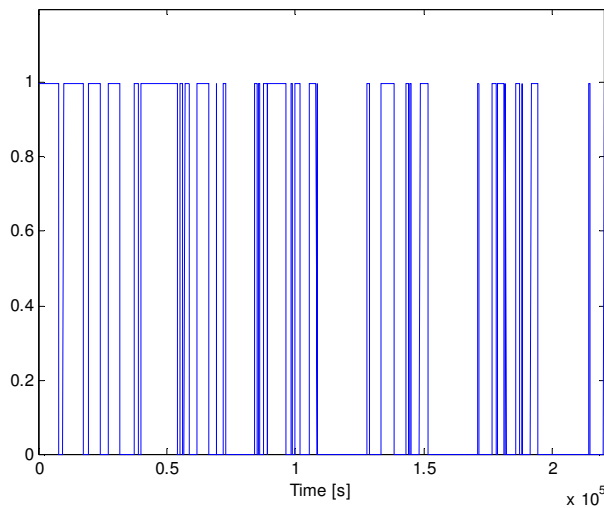


Figure 8 – Visibility flag (20dB-Hz threshold case)

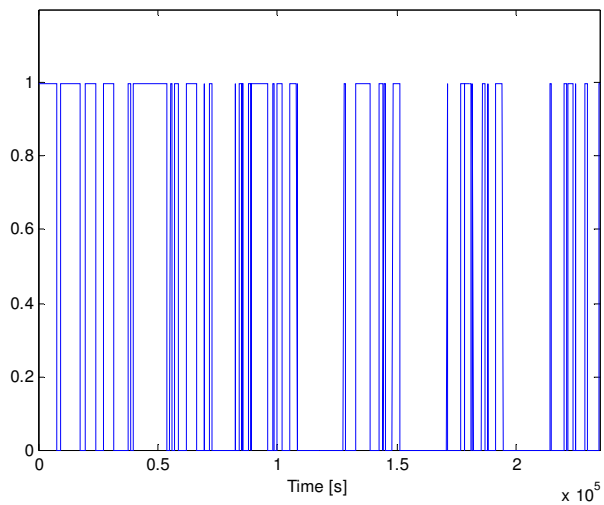


Figure 9 – Visibility flag (20dB-Hz threshold case)

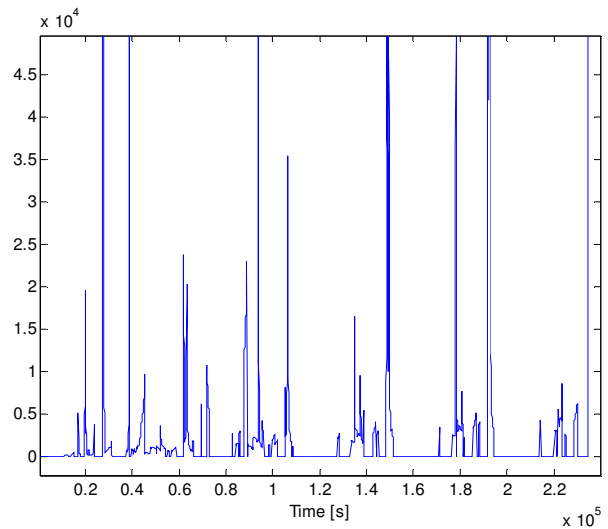


Figure 10 – GDOP behavior during lunar transfer computed for the 15dB-Hz SNR acquisition threshold case.

for both velocity and positions (to initialize the covariance matrix) are definitely better, due to low GDOP conventional geometry which is easy to match in the parking orbit.

Figures 7-8-9 report the visibility flag (1 in view / 0 outages) for three different threshold acquisition. The more capable case obviously includes the previous ones. However, even the 15dB-Hz case definitely leaves a number of signal-empty intervals, where no measurements will be available. Figure 10 shows the behaviour (really different from land or traditional space – LEO – applications) of the GDOP, which includes exceptionally high values. Note that value during outages has been zeroed.

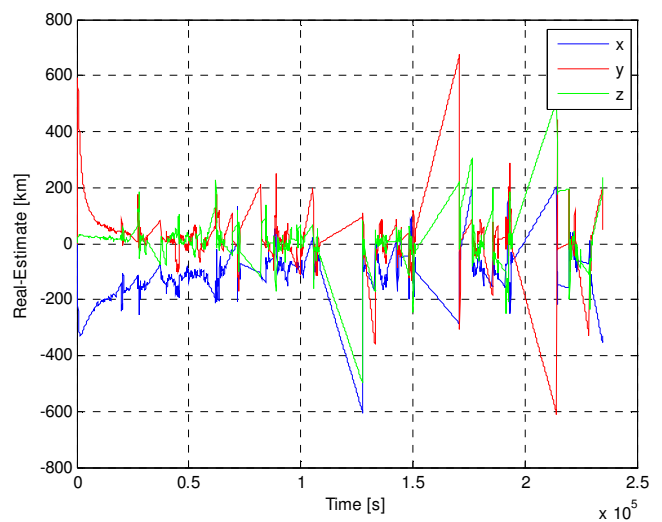


Figure 11 – Errors on the position components of the kinematic state provided by UKF application.

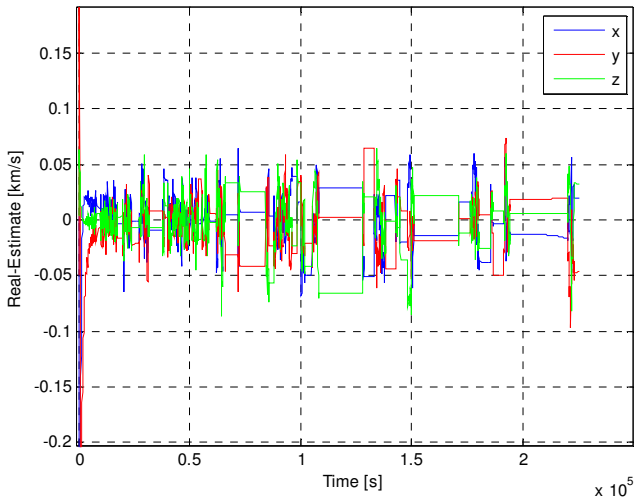


Figure 12 – Errors on the velocity components estimation for a 30 dB-Hz acquisition threshold accepted in signal processing.

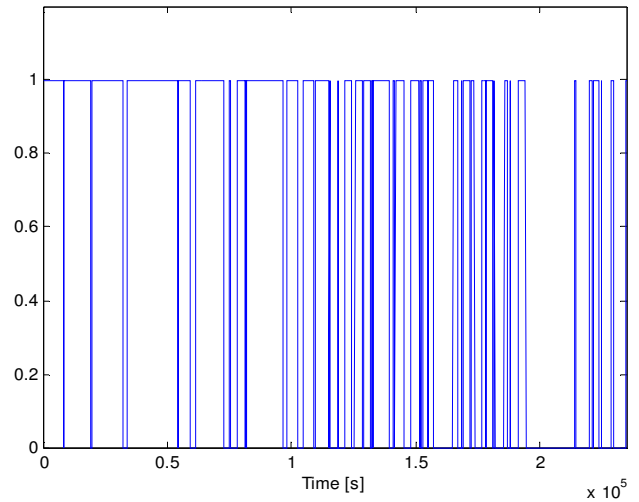


Figure 15 – Visibility flag during the direct transfer with a pseudosatellite located on the Moon.

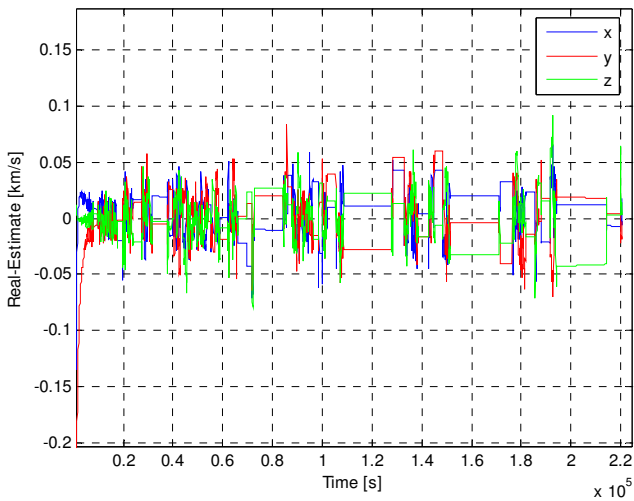


Figure 13 – Errors on the velocity components estimation for a 20 dB-Hz acquisition threshold accepted in signal processing.

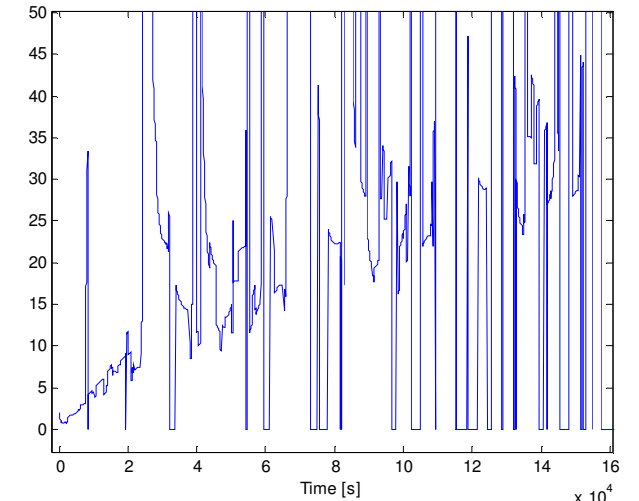


Figure 16 – Detail of the GDOP during the direct transfer with a pseudosatellite located on the Moon.

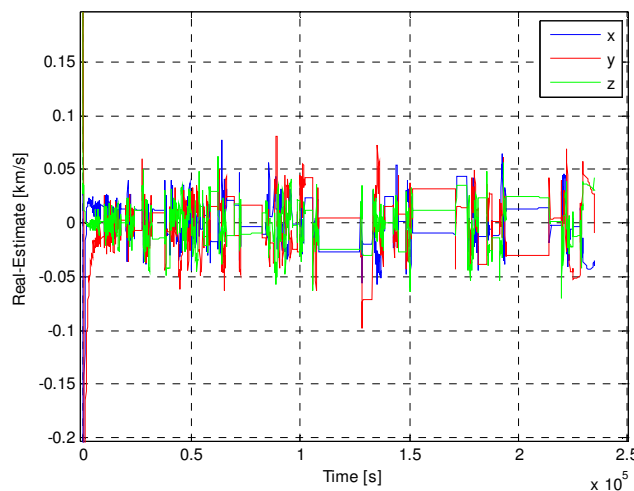


Figure 14 – Errors on the velocity components estimation for a 15 dB-Hz acquisition threshold accepted in signal processing.

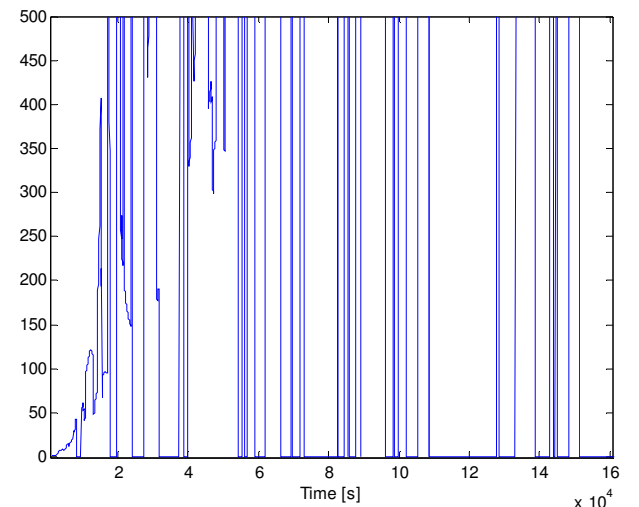


Figure 17 – Detail of the GDOP during the direct transfer without lunar pseudosatellite to augment the GNSS sources constellation.

Figure 11 plots the error of the estimation on position components provided by the estimator (UKF) with respect to the simulated dynamics, which represents the true one. It is easy to remark how the error grows when fixes are unavailable (specifically note the intervals at about $1.3 \cdot 10^5$ s, immediately past $1.5 \cdot 10^5$ s and around $2 \cdot 10^5$ s). Caution should be used to provide a quantitative meaning to these figures, as the filter should be carefully tuned to the specific task.

Figures 12-13-14 refer to velocity components estimates, which are clearly important in order to assess the magnitude of possible correction manoeuvres. Sets are referred to decreasing thresholds accepted for signal acquisition. The comparison among these results shows the gain due to data processing that, even if enabling marginally longer intervals, contributes so doing in limiting the divergence of outage periods.

It is difficult to think about dramatic improvement based on acquiring more satellites, i.e. further lowering the acquisition threshold. The limit is represented by the poor observation geometry, which reduces the benefits of the GNSS fixes carried out during the (definitely not negligible) visibility intervals. Several studies considered the possibility to help navigating interplanetary missions by locating beacons on the surface of the targeted planetary body. In lunar case, such a beacon, which is going to act as a pseudosatellite, has the strong advantage to constantly face the Earth, therefore making easier its control/command form the Earth. The largest operational issue is represented by its survival, even in a sleeping mode, during periodic lunar night.

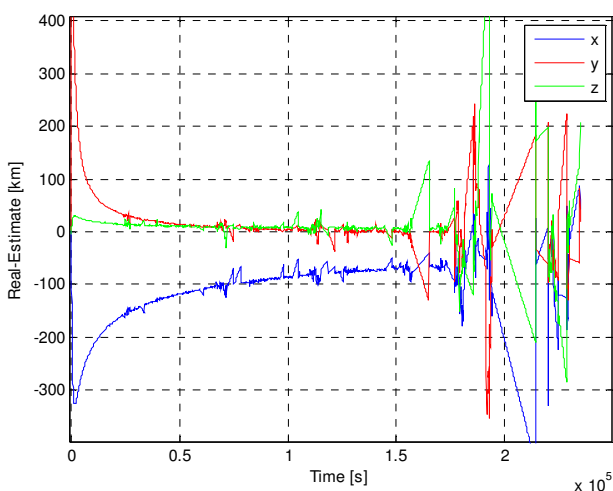


Figure 18 – Errors on the position components for a 20 dB-Hz threshold for useful signal processing in case of a pseudosatellite located on the Moon.

Following figures show the improvement granted by a single pseudosatellite, which is supposed to be located on the Moon equator, at the closest point from Earth. Figure 15, concerning the visibility flag, highlights how the outages during the cruise phase are remarkably shortened. Even more important, the geometry is noticeably improved, as proofed by figure 16. In fact, Figure 17 (a zoom of previous figure 10) which is referred to the case without pseudosatellite and reported for comparison, shows a behavior far worse, with already recalled large GDOP values. Instead, the plot in Figure 16 indicates an almost linear trend, with values not higher than one order of magnitude than typical LEO's ones. Notice that sudden increases in GDOP could be efficiently managed by the filter, as it happens with short duration outages, represented in the plot by zeroed GDOP.

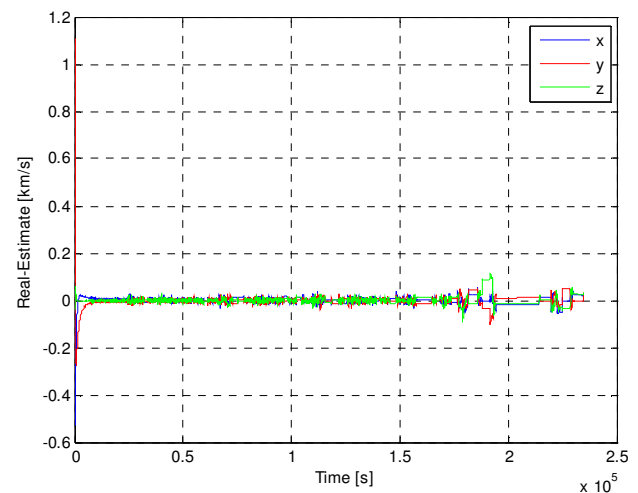


Figure 19 – Errors on the velocity components for a 20 dB-Hz acquisition threshold in signal processing in case of a pseudosatellite located on the Moon.

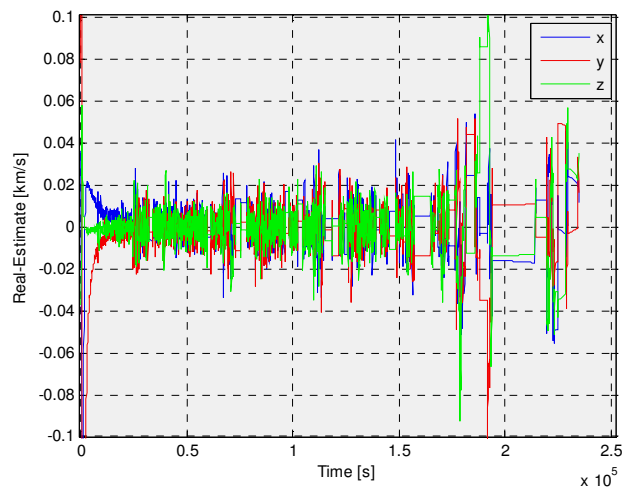


Figure 20 – Errors on the velocity components for a 20 dB-Hz threshold for useful signal processing in case of a pseudosatellite located on the Moon (detail)

Figure 18 shows the performance in terms of position errors, while Figures 19 and 20 refer to velocity components, offering a quite remarkable improvement with respect to the case without the lunar pseudosatellite. Note that such an advantage in performance is gained all along the path, and that to maintain the estimate quite close to the true pays later, when the spacecraft, next to the Moon, loses the pseudosatellite visibility. Of course, this case should be further ameliorated by including more than one pseudosatellite, a strategy to be considered if a continuing exploration should be pursued.

REMARKS AND OVERVIEW OF FURTHER DEVELOPMENTS

The interest for extending GNSS use for autonomous inboard orbit determination to altitudes higher than the constellation's one is clear and soundly motivated. Future lunar missions, even if probably at the extreme feasibility boundary for this technique, are a possible application area. A number of studies have been published on the subject, and the present one adds new simulation results relevant to lower sensitivity threshold which should be possible by heavy data processing technique to be applied in the signal digital processing. Such a signal processing will be almost certainly carried out by software receivers, which allow to repeatedly process a long batch of data with several correlation techniques until "mining" the GNSS code. The drawback, i.e. the lack of real time performance and/or the high computation cost, should be negotiated in the perspective of a discontinuous availability of the fix, which is a completely acceptable feature in this application.

Main relevance of the results presented in this paper stay in the performance which can be attained at the Moon by linking observation (from a poor geometry), acquisition (with a good "digital" sensitivity) and estimation (with easy dynamic modelling). The approach should be still improved – from the astrodynamist's point of view – by: 1) generalization of the trajectory considered for direct transfer, possibly including out-of-plane manoeuvres and different lunar entry scenarios, and 2) extension to the low thrust spiralling trajectory (a theme preliminarily faced in [7]).

From the signal point of view, the inclusion of future GNSS systems as additional sources to the GPS will be considered, even if the nature of the solution improvement trend, at least for Galileo case, has been already assessed in [7]. Also, new systems could include new signals ("pilot"), able to

make easier the analysis of signal intervals longer than the 1 data message bit which is currently a kind of constraint for GPS. This possibility will be investigated in [12]. Again on signal issues, test of the algorithms proposed in [9] should be actually carried out within a (still simulated) dynamic environment as the one represented by the proposed trajectories (in fact, presented research accepted the acquisition thresholds as granted, but explicit test with lunar transfer case will add further confidence).

From the point of view of the system general design, the promising addition of lunar pseudosatellites should be better investigated, including several pseudosatellites and different locations. Moreover, the effect of such a solution in order to navigate also the lunar parking orbit (or the selected scientific/observation orbit), a portion of which will be over the dark side, should be looked at. Techniques to command and synchronize the pseudosatellites, in addition to their operational (thermal and power budgets) issues, will need some attention.

Probably the most important and immediate aspect to be analysed deals with the estimation phase. In fact, while this paper, as well as reference [8], show that a fixing spaced out by outages can be managed by the adoption of filters including a propagation step, the filter itself should be tailored to the specific application. UKF architecture seems the right choice in order to easily integrate additional perturbations, like solar radiation pressure, even if the improvement in dynamic modelling should be expected to provide more confidence on the results better than remarkably change the path. Tuning of process and measurements noise matrices will be instead the main upcoming task, in order to correctly represent the different conditions along the transfer.

REFERENCES

- [1] S.C.Wu *et al.*, "MicroGPS for Low-Cost Orbit Determination", TDA Progress Report 42-131, 1997.
- [2] E. Imre, P. Palmer, Y. Hashida, "Precise Relative Orbit Determination for Low Earth Orbit Formation Flight Using GPS Pseudo-range and Carrier-Phase Measurements", 16th AIAA/USU Conference on Small Satellites, 2002.
- [3] C.C. Chao, H. Bernstein, "Onboard Stationkeeping of Geosynchronous Satellite Using a Global Positioning System Receiver", Journal of Guidance, Control, and Dynamics, Vol. 17, No. 4, 1994.

- [4] J.L.Ruiz, C.H. Frey, “*Geosynchronous Satellite Use of GPS*”, ION GNSS-18, Long Beach (CA, USA), 2005.
- [5] O.Balbach, B.Eissfeller, G.Hein, W.Enderle, M. Schmidhuber, N.Lemke, “*Tracking GPS above GPS Satellite Altitude: First Results of the GPS Experiment on the HEO Mission Equator-S*”, Proceedings of the IEEE PLANS, pp. 243-249, 1998.
- [6] G.Davis, M.Moreau, F.Bauer, J.R. Carpenter, “*GPS Based Navigation and Orbit Determination for the AMSAT AO-40 Satellite*”, AIAA Guidance and Control Conference, Monterey (USA), 2002.
- [7] G.B.Palmerini, M.Sabatini, G.Perrotta “*En Route to the Moon Using GNSS Signals*”, *Acta Astronautica*, vol 64, No.4, pp.467-483 (2009).
- [8] G.B.Palmerini, M.Sabatini, F.Reali “*Navigation Techniques for Microsatellites targeted to the Moon*”, paper IAF-08-B.4.8.9, Proc. International Astronautical Congress, Glasgow, 2008.
- [9] N.I. Ziedan, “*GNSS Receivers for Weak Signals*”, Artech House, Norwood (MA, USA), 2006.
- [10] R.R. Bate, D.D. Mueller, J.E. White, *Fundamentals of Astrodynamics*, Dover Publications, New York, 1971.
- [11] ESA - European Space Agency, “*European Student Moon Orbiter [ESMO] Project - Statement of Work for Phases B1/B2/C/D/E1*”, Appendix 1 to ITT 1-6031/09/NL/NA, released 16/3/2009.
- [12] F.Rodriguez, G.B.Palmerini “*En Route to the Moon Using GNSS Signals*”, proposed abstract for the ION GNSS Conference, Savannah (GA, USA), September 2009.
- [13] S.J. Julier, J.K. Uhlmann, H.F. Durrant-Whyte, “*A New Approach for Filtering Nonlinear Systems*”, Proceedings of the American Control Conference, Seattle (WA, USA), pp. 1628-1632, 1995.